

# Interaction of the $[\text{GaH}_4]^-$ Anion with Weak XH Acids – A Spectroscopic and Theoretical Study

Natalia V. Belkova,<sup>[a]</sup> Oleg A. Filippov,<sup>[a]</sup> Andrey M. Filin,<sup>[a]</sup> Liliya N. Teplitskaya,<sup>[a]</sup>  
Yulia V. Shmyrova,<sup>[a]</sup> Vyacheslav V. Gavrilenko,<sup>[a]</sup> Ludmila M. Golubinskaya,<sup>[a]</sup>  
Vladimir I. Bregadze,<sup>[a]</sup> Lina M. Epstein,<sup>\*,[a]</sup> and Elena S. Shubina<sup>\*,[a]</sup>

**Keywords:** Hydrides / Hydrogen bonding / IR spectroscopy / Theoretical methods / Boron / Gallium

The dihydrogen bonding (DHB) between the hydride atom of the  $[\text{Bu}_4\text{N}][\text{GaH}_4]$  salt and different XH acids, namely  $\text{CF}_3\text{CH}_2\text{OH}$ ,  $\text{FCH}_2\text{CH}_2\text{OH}$ ,  $i\text{PrOH}$ ,  $\text{MeOH}$ , indole and  $4\text{-O}_2\text{NC}_6\text{H}_4\text{NH}_2$ , has been investigated for the first time by low-temperature IR spectroscopy. The DHB spectroscopic and thermodynamic parameters in solvents of low polarity and high basicity ( $E_j = 1.37$ ) were obtained. The nature, structures, energies and electron distributions of the model DHB complexes of  $\text{GaH}_4^-$  with  $\text{H}_2\text{O}$ ,  $\text{MeOH}$ ,  $\text{CF}_3\text{OH}$ ,  $\text{H}_2\text{NCF}_3$  or  $\text{NO}_2\text{C}_6\text{H}_4\text{NH}_2$  were studied by DFT calculations and compared with those of the analogous complexes of  $\text{BH}_4^-$  with  $\text{H}_2\text{O}$ ,  $\text{MeOH}$  or  $\text{CF}_3\text{OH}$ . Two types of DHB struc-

tures with monodentate and symmetric chelate coordination were found. The lengthening of the X–H and Ga–H bonds, electron polarization and overlap population of the  $\text{H}\cdots\text{H}$  bond are greater in the first type of structure. A comparative analysis of experimental data demonstrates that the spectroscopic and thermodynamic characteristics, e.g.  $\nu(\text{XH})$  and  $\nu(\text{GaH})$  band shifts,  $\nu(\text{XH})_{\text{bonded}}$  integral intensities, formation enthalpies and  $E_j$  of all the DHB complexes increase down the group ( $\text{BH}_4^-\cdots\text{HX} < \text{GaH}_4^-\cdots\text{HX}$ ).

(© Wiley-VCH Verlag GmbH & Co. KGaA, 69451 Weinheim, Germany, 2004)

## Introduction

The unconventional intermolecular hydrogen bond between XH proton donors and the hydride ligands of transition metal hydride complexes ( $\text{XH}^{\delta+}\cdots\text{H}^{\delta-}\text{M}$ ) were discovered between 1995 and 1996 and have been actively investigated since this time with several reviews appearing on the topic.<sup>[1–6]</sup> The formation conditions, structural and energetic characteristics of these unusual hydrogen bonds were determined by low-temperature IR and NMR spectroscopy in solution and by X-ray and neutron diffraction in the solid state. A variety of theoretical methods were devoted to the nature and structure of this dihydrogen bond (DHB) formed by transition metal hydrides in the gas phase.<sup>[1,5,7,8]</sup> It has been shown that these  $\text{H}\cdots\text{H}$  complexes are important intermediates in proton transfer reactions leading to transition metal dihydrogen complexes.<sup>[1,6,9–11]</sup> In very recent DFT work,<sup>[11]</sup> the solvent was introduced by a polarizable continuum model and its stabilising effect on the protonation process was studied.

The ability of main group element hydrides to form DHBs was studied for the first time using boron hydrides.<sup>[12–17]</sup> An analysis of the structures from the Cambridge Structural Database and theoretical calculations on

the dimer  $(\text{BH}_3\text{NH}_3)_2$  led to the conclusion that the DHB moiety is significantly bent.<sup>[12,13]</sup> Later, our IR investigations in solution combined with theoretical studies of the  $(\text{H}_3\text{NBH}_3)_2$  dimer as well as the DHB of  $\text{BH}_4^-$  and  $\text{BH}_3\text{NH}_3$  with proton donors ( $\text{H}_2\text{O}$ ,  $\text{MeOH}$  and  $\text{HCN}$ ) led to the conclusion that substantial deviations from linearity in the solid state are caused by the crystalline packing.<sup>[14,15]</sup> The linearity of the  $(\text{B})\text{H}\cdots\text{HX}$  moiety and reasonable electron density changes have been demonstrated by theoretical calculations of  $(\text{H}_3\text{NBH}_3)_2$  using the RHF/6-31G<sup>[15]</sup> and A1M<sup>[16]</sup> methods, though the nonlinear bifurcated DHB (of  $\text{C}_{2v}$  symmetry) was reported in previous works (HF, DFT, MP2 methods).<sup>[17]</sup> Recently, neutron diffraction measurements corrected the “heavy” atom assignments for  $(\text{H}_3\text{NBH}_3)_2$  leading to the structure with practically linear  $\text{NH}\cdots\text{H}(\text{B})$  DHBs and bent  $\text{BH}\cdots\text{H}(\text{N})$  moieties.<sup>[18]</sup> The similarity between  $\text{BH}\cdots\text{HX}$ ,  $\text{MH}\cdots\text{HX}$  and classical H bonds in the structure was established.<sup>[1,6,15]</sup> Recently, some reports have been devoted to theoretical DHB calculations of the other main group hydride complexes  $\text{EH}\cdots\text{HX}$ .<sup>[19–21]</sup> A theoretical study of DHB complexes between some simple hydrides (for example,  $\text{BeH}_2$ ,  $\text{MgH}_2$ ,  $\text{SiH}_4$ ,  $\text{GeH}_4$  and  $\text{SnH}_4$ ) and HF showed a correlation between  $\text{H}\cdots\text{H}$  distances and the energies of the DHB.<sup>[22]</sup> Cyclotriallumozane  $(\text{NH}_2\text{AlH}_2)_3$  was found theoretically to have a favourable twist-boat conformation in the gas phase with two  $\text{H}\cdots\text{H}$  interactions.<sup>[23]</sup> A comparison of the calculated structures and energies of  $\text{NH}\cdots\text{HE}$  ( $\text{E} = \text{B}, \text{Al}, \text{Ga}$ ) for  $(\text{NH}_3\text{EH}_3)_2$  predicted  $\text{C}_2$  symmetry for the dimers of the Al and Ga

<sup>[a]</sup> A. N. Nesmeyanov Institute of Organoelement Compounds, Russian Academy of Sciences, Vavilov str. 28, 119991 Moscow, Russia  
Fax: (internat.) + 7-095-135-5085  
E-mail: shu@ineos.ac.ru

hydrides and the DHB energy was shown to decrease down the group.<sup>[17]</sup>

It is noteworthy that experimental studies of Al and Ga hydrides have considered only the structures of the crystalline adducts.<sup>[20]</sup> An intramolecular  $\text{NH}\cdots\text{HAl}$  hydrogen bond was determined from an X-ray diffraction study of the alane–piperidine complex<sup>[24]</sup> and six short  $\text{H}\cdots\text{H}$  contacts were found in the structure of the  $[(\text{NH}_2\text{AlH}_2)_3]_2$  dimer.<sup>[23]</sup> The neutron diffraction crystal structure of cyclotri-galozane  $(\text{NH}_2\text{GaH}_2)_3$  indicated self-assembly from four  $\text{NH}\cdots\text{HGa}$  dihydrogen bonds.<sup>[23]</sup> To date, there is no evidence for the existence of  $\text{GaH}\cdots\text{HX}$  interactions in solution. However, DHB interactions are very important allowing control over reactivity and selectivity in solution. This has potential implications in catalysis and promises an important role in the creation of supramolecular assemblies and new covalent materials.<sup>[1,20]</sup>

In this work we present the results of a VT-IR investigation (190–290 K) including spectroscopic and thermodynamic characteristics of DHB formed in low-polarity solvents between  $\text{GaH}_4^-$  (**1**) and proton donors of different strength, i.e.  $\text{CF}_3\text{CH}_2\text{OH}$ ,  $\text{FCH}_2\text{CH}_2\text{OH}$ , *i*PrOH, MeOH, indole and 4- $\text{O}_2\text{NC}_6\text{H}_4\text{NH}_2$ . VT-IR spectroscopy, as has been previously shown, is a very convenient method for studying DHB complexes providing not only evidence of the formation of DHB, but also allowing the detection of the separate bands of the initial and H-bonded complexes. The technique also enables determination of the formation energy.<sup>[6,15]</sup>

The nature, structures, energies and electron distributions of the model DHB complexes formed between **1** and  $\text{H}_2\text{O}$ , MeOH,  $\text{CF}_3\text{OH}$ ,  $\text{H}_2\text{NCF}_3$  or 4- $\text{O}_2\text{NC}_6\text{H}_4\text{NH}_2$  are discussed on the basis of ab initio calculations and compared with those of analogous complexes of  $\text{BH}_4^-$  with  $\text{H}_2\text{O}$ , MeOH, or  $\text{CF}_3\text{OH}$ .

## Results and Discussion

### Spectroscopic Evidence for Hydrogen Bonding in Solution

The IR spectra of OH and NH acids (in the concentration range of  $10^{-2}$  to  $10^{-3}$  M in order to exclude self-association) were measured in dichloromethane with an excess of gallohydride **1**. The intensities of the  $\nu(\text{XH})$  stretch-

ing vibrations decrease in the presence of **1** and new, lower frequency broad bands ( $3392\text{--}3224\text{ cm}^{-1}$ ) of H-bonded XH groups [ $\nu(\text{XH})_{\text{bonded}}$ ] appear (e.g. Figure 1). This pattern demonstrates formation of hydrogen bonds between proton donors and the gallium hydride. The intensities of the  $\nu(\text{XH})_{\text{bonded}}$  bands increase as the temperature decreases as illustrated in Figure 1 for MeOH. This indicates the right shift for the H-bonding equilibrium upon cooling.

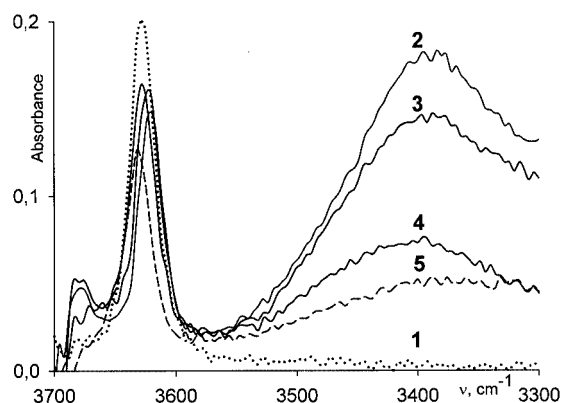


Figure 1. IR spectra in the  $\nu(\text{OH})$  range of MeOH ( $c = 0.015$  M,  $\text{CH}_2\text{Cl}_2$ ) at 260 K (1); in the presence of  $[\text{Bu}_4\text{N}]\text{GaH}_4^-$  (0.09 M): at 200 K (2); 220 K (3); 260 K (4); 290 K (5)

All spectroscopic parameters, i.e. frequency shifts  $[\Delta\nu(\text{XH}) = \nu(\text{XH})_{\text{free}} - \nu(\text{XH})_{\text{bonded}}]$ , half-widths of the  $\nu(\text{XH})_{\text{bonded}}$  bands ( $\Delta\nu_{1/2}$ ) and integral intensities  $[A(\text{XH})_{\text{bonded}}]$  increase with the increase of the proton-donating ability of XH in the following sequence: 4- $\text{O}_2\text{NC}_6\text{H}_4\text{NH}_2 < i\text{PrOH} < \text{MeOH} < \text{FCH}_2\text{CH}_2\text{OH} \approx \text{C}_6\text{H}_5\text{NH} < \text{CF}_3\text{CH}_2\text{OH}$ . The values of  $\Delta\nu(\text{XH})$  increase along this series from 144 to  $250\text{ cm}^{-1}$ ,  $A(\text{XH})_{\text{bonded}}$  increases from  $5.12 \times 10^4$  to  $9.52 \times 10^4\text{ L}\cdot\text{cm}^{-2}\cdot\text{mol}^{-1}$  and  $\Delta\nu_{1/2}$  increases from 97 to  $287\text{ cm}^{-1}$  (Table 1).

Interesting results were obtained from the study of the  $\text{GaH}_4^-/4\text{-O}_2\text{NC}_6\text{H}_4\text{NH}_2$  system in  $\text{CH}_2\text{Cl}_2$  solution. Two bands of the  $\text{NH}_2$  group of 4- $\text{O}_2\text{NC}_6\text{H}_4\text{NH}_2$  in the IR spectra can be assigned to asymmetrical ( $\nu^{\text{as}} = 3509\text{ cm}^{-1}$ ) and symmetrical ( $\nu^{\text{s}} = 3411\text{ cm}^{-1}$ ) stretching vibrations. In the presence of the anion **1**, two new bands (3481 and  $3337\text{ cm}^{-1}$ )

Table 1. Spectroscopic characteristics of the hydrogen-bonded complexes of XH acids to  $\text{GaH}_4^-$

HX	$\nu(\text{XH})_{\text{free}}$ [ $\text{cm}^{-1}$ ]	$\nu(\text{XH})_{\text{bond}}$ [ $\text{cm}^{-1}$ ]	$\Delta\nu(\text{XH})$ [ $\text{cm}^{-1}$ ]	$\Delta\nu_{1/2}$ [ $\text{cm}^{-1}$ ]	$A(\text{XH})_{\text{bond}} \times 10^4$ [ $\text{L}\cdot\text{cm}^{-2}\cdot\text{mol}^{-1}$ ]
4- $\text{NO}_2\text{C}_6\text{H}_4\text{NH}_2$	3509(as) 3411(s)	3481 <sup>[a]</sup> 3337 <sup>[a]</sup>	123 <sup>[b]</sup>	68 <sup>[c]</sup>	5.12 <sup>[c]</sup>
Indole	3473	3224	249	132	7.33
<i>i</i> PrOH	3604	3392	212	219	—
$\text{CH}_3\text{OH}$	3619	3393	226	189	6.23
$\text{FCH}_2\text{CH}_2\text{OH}$	3605	3369	236	235	7.67
$\text{CF}_3\text{CH}_2\text{OH}$	3600	3350	250	287	9.52

<sup>[a]</sup> New bands, assignments are discussed in the text. <sup>[b]</sup> Mean of  $\nu^{\text{as}}$  and  $\nu^{\text{s}}$  bands of free 4-nitroaniline was used as  $\nu(\text{XH})_{\text{free}}$  for  $\nu(\text{XH})$  calculation. <sup>[c]</sup> For the band at  $3337\text{ cm}^{-1}$ .

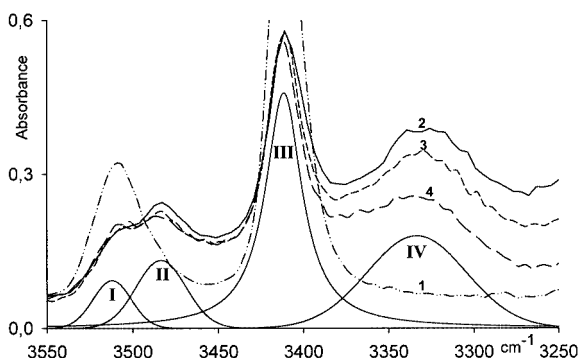


Figure 2. IR spectra in the  $\nu(\text{NH})$  range of  $4\text{-O}_2\text{NC}_6\text{H}_4\text{NH}_2$  ( $c = 0.02$  M,  $\text{CH}_2\text{Cl}_2$ ) at 200 K (1); in the presence of  $[\text{Bu}_4\text{N}]\text{GaH}_4^-$  (0.09 M): at 200 K (2); 230 K (3); 250 K (4) and separation of the band (2) on the four components:  $\nu(\text{NH})^{\text{as}}$  (I),  $\nu(\text{NH})^{\text{as}}$  (III) and II, IV (see text for assignment)

cm<sup>-1</sup>) appear and grow upon cooling (Figure 2). There are two possibilities for the assignments of these two bands. In the case of monodentate coordination, these bands could be attributed to the free and bonded species, respectively. In the case of bidentate coordination, these bands would correspond to the  $\nu^{\text{as}}$  and  $\nu^{\text{s}}$  bands of the bonded species. Analysis of the IR spectra and band separation enables us to suggest the first type of assignment.<sup>[25]</sup> The new high-frequency band  $\nu(\text{NH})$  at 3481 cm<sup>-1</sup> is narrow ( $\Delta\nu_{1/2} = 34$  cm<sup>-1</sup>) and the second new band at 3337 cm<sup>-1</sup> is much broader ( $\Delta\nu_{1/2} = 68$  cm<sup>-1</sup>). Shifts of these bands corresponding to  $[\nu(\text{NH})^{\text{as}} + \nu(\text{NH})^{\text{s}}]/2$  are -21 and 123 cm<sup>-1</sup>, respectively. Taking into account both factors, we can assign these bands as  $\nu(\text{NH})_{\text{free}} = 3481$  cm<sup>-1</sup> and  $\nu(\text{NH})_{\text{bond}} = 3337$  cm<sup>-1</sup>. The results of theoretical calculations (see below) confirm both the monodentate coordination and this assignment.

Spectroscopic evidence for the hydride ligand being the site of DHB formation was obtained from a range of Ga–H stretching vibrations studied in THF at 180–290 K. It was shown earlier that DHB formation results in a low-frequency shift of the M–H or B–H stretches for the groups participating in H-bonding, whereas the bands corresponding to the groups that do not participate in H-bonding shift to the high-frequency region.<sup>[6,15]</sup> Thus, the formation of GaH...HX bonds, leads to some broadening of the  $\nu(\text{GaH})$  band accompanied by the appearance of low-frequency and high-frequency shoulders assignable to stretching vibrations of the one bonded and three free GaH bonds, respectively. Such changes were observed in the interaction with the weakest proton donor used, i.e. 4-O<sub>2</sub>NC<sub>6</sub>H<sub>4</sub>NH<sub>2</sub> (Figure 3). The band intensity of **1**,  $\nu(\text{GaH}) = 1700 \text{ cm}^{-1}$ , decreases and the stretching vibrations of the free GaH groups in the DHB complex are displaced to the high-frequency range. Those of the GaH-bonded group appear as the low-frequency shoulder.

One could expect more pronounced changes for stronger XH acids, as in the case of the  $\text{BH}_4^-/(\text{CF}_3)_2\text{CHOH}$  system.<sup>[15]</sup> However, less pronounced changes were observed in the IR spectra of **1** in the presence of  $\text{FCH}_2\text{CH}_2\text{OH}$  and indole at 200 K. Moreover, the  $\nu(\text{GaH})$  band intensity de-

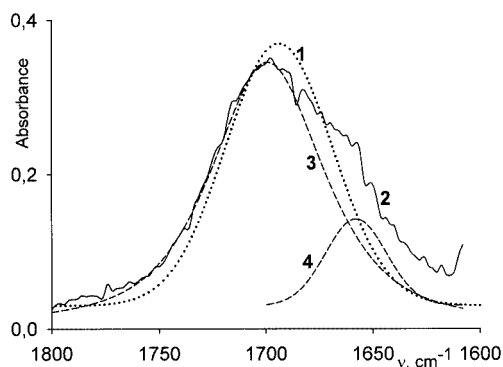


Figure 3. IR spectra in the  $\nu(\text{GaH})$  range of  $[\text{Bu}_4\text{N}]\text{GaH}_4^-$  ( $c = 0.03 \text{ M}$ , THF) at 200 K (1); in the presence of 4- $\text{O}_2\text{NC}_6\text{H}_4\text{NH}_2$  (0.08 M) at 200 K (2); separation of the band (2) on the two components:  $\nu(\text{GaH})_{\text{free}}$  (3) and  $\nu(\text{GaH})_{\text{bonded}}$  (4)

creases as the temperature increases ( $> 240$  K) probably due to proton transfer with subsequent  $\text{H}_2$  gas evolution and formation of covalent Ga–O/Ga–N bonds. We have not yet studied this process in more detail, but there are many examples of boron hydride alcoholysis/hydrolysis studies in the literature, e.g. the  $\text{BH}_4^-/\text{R}^f\text{OH}^{[26]}$  and  $\text{GaH}_4^-/\text{ROH}^{[27]}$  systems. However, the  $\text{H}\cdots\text{H}$  bonding was not considered as an intermediate along the reaction pathway. By analogy with transition metal hydrides,<sup>[6]</sup> we suggest Scheme 1 for the reaction with alcohols where the proton transfer from DHB complexes leads to nonclassical ( $\eta^2\text{-H}_2$ ) complex formation followed by hydrogen elimination yielding alkoxy derivatives. Evidently, the ( $\eta^2\text{-H}_2$ ) complexes of **1** should be very unstable as for other main group element hydrides, but the data concerning the theoretical and experimental evidence of the boron analogue<sup>[28]</sup> (IR spectra in cryogenic matrices at 13–27 K) support our hypothesis.



Scheme 1

The participation of more alcohol molecules in the reaction generates alkoxy products of different compositions,  $[\text{H}_{4-n}\text{Ga}(\text{OR})_n]^-$ .<sup>[27]</sup> The same is true of the aminolysis reactions. The reaction can stop at the first step of DHB intermediate formation, depending on temperature and the amount and strength of the proton donor. The interaction with weakest XH acid used (4-nitroaniline), as mentioned above, does not lead to proton transfer and  $\text{H}_2$  evolution in the temperature range of 180–250 K. IR spectroscopic changes demonstrate only DHB formation (equilibrium  $\mathbf{1} \rightleftharpoons \mathbf{2}$ ; Scheme 1). The temperature dependence is reversible. The interaction with the stronger  $\text{FCH}_2\text{CH}_2\text{OH}$  or indole leads to the reduction of the  $\nu(\text{GaH})$  intensity at 230 K and to practically full disappearance of this band at ambient temperature. At the same time, a very broad and high frequency absorbance ( $1800\text{--}1850\text{ cm}^{-1}$ ) appears which probably corresponds to the Ga–H stretching of different al-

coholysis or aminolysis products (**4** in Scheme 1). The same spectroscopic changes were observed in the interaction with the stronger OH acid  $\text{F}_3\text{CCH}_2\text{OH}$  (Figure 4, line 2). In this case, some decrease in the  $\nu(\text{GaH})_{\text{free}}$  band intensity ( $1700\text{ cm}^{-1}$ ) of the DHB complex took place even at low temperature (200 K) with the simultaneous appearance of the broad high-frequency absorbance. Upon a temperature change from 200 to 290 K, broad overlapping bands ( $1763\text{ cm}^{-1}$  at 200 K and  $1810\text{ cm}^{-1}$  at 290 K) increased irreversibly (Figure 4). Moreover, the intensity of these bands increased concomitantly with the decrease of the  $\nu(\text{GaH})_{\text{free}}$  band (Figure 4). These can be tentatively assigned to the  $\nu(\text{GaH})$  vibrations of  $[\text{GaH}_{4-n}(\text{OCH}_2\text{CF}_3)_n]^-$ .<sup>[27]</sup> However, a special study is necessary in order to obtain the data corresponding to the spectroscopic changes during the alcoholysis/aminolysis reactions and definite assignment of each band.

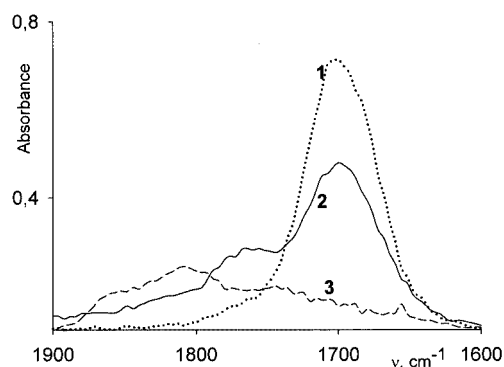


Figure 4. IR spectra in the  $\nu(\text{GaH})$  range of  $[\text{Bu}_4\text{N}]\text{GaH}_4^-$  ( $c = 0.04\text{ M}$ , THF) at 200 K (1); in the presence of TFE (0.10 M): at 200 K (2); at 290 K (3)

It should be noted that the  $\Delta\nu(\text{GaH})$  values of the DHB complexes of **1** with weak proton donors are  $10\text{--}30\text{ cm}^{-1}$  larger than the  $\Delta\nu(\text{BH})$  values for the analogous DHB complexes of  $\text{BH}_4^-$ .<sup>[15]</sup> The changes in the spectroscopic characteristics of the XH acids in the presence of **1**, such as  $\nu(\text{XH})$  band shifts,  $\nu(\text{XH})_{\text{bonded}}$  band half-widths ( $\Delta\nu_{1/2}$ ) and integral intensities ( $A$ ), are also higher than those in the presence of  $\text{BH}_4^-$ .

### Strength of $\text{GaH}\cdots\text{HX}$ Bonds

The enthalpies ( $-\Delta H$ ) of the  $\text{GaH}\cdots\text{HX}$  bond formations were determined from the empirical correlation Equations (1) and (2). These were proposed by Iogansen for classical H-bonded systems<sup>[29–31]</sup> but have also proved to be valid for dihydrogen bonds to transition metal<sup>[6]</sup> and boron hydrides.<sup>[15]</sup>

$$-\Delta H^\circ = 18 \times \Delta\nu/720 + \Delta\nu \quad (1)$$

$$-\Delta H^\circ = 2.9(\Delta A)^{1/2} \quad (2)$$

The enthalpy values of dihydrogen-bonded complex formation obtained from frequency shifts [Equation (1)] and integral intensity changes [Equation (2)] have similar values

Table 2. The enthalpy values of DHB complexes [ $\text{kcal}\cdot\text{mol}^{-1}$ ] of  $\text{GaH}_4^-$  (**1**) and  $P_i$  factors of proton donors<sup>[29]</sup>

HX	$-\Delta H^\circ$ [a]	$-\Delta H^\circ$ [b]	$P_i$ [29]
4- $\text{O}_2\text{NC}_6\text{H}_4\text{NH}_2$	2.6	—	0.41
Indole	4.4	4.5	0.75
<i>i</i> PrOH	4.0	—	0.58
$\text{CH}_3\text{OH}$	4.3	4.1	0.63
$\text{FCH}_2\text{CH}_2\text{OH}$	4.4	4.7	0.74
$\text{CF}_3\text{CH}_2\text{OH}$	5.4	5.2	0.89

[a]  $-\Delta H^\circ$  calculated using Equation (1). [b]  $-\Delta H^\circ$  calculated using Equation (2).

as is apparent from Table 2. The  $\text{GaH}\cdots\text{HX}$  bond energies correspond to medium-strength H bonds:  $-\Delta H^\circ$  values of the DHB complexes change from 4.0 to  $5.4\text{ kcal}\cdot\text{mol}^{-1}$  with the exception of the weak DHB to 4- $\text{O}_2\text{NC}_6\text{H}_4\text{NH}_2$  ( $2.6\text{ kcal}\cdot\text{mol}^{-1}$ ).

The proton accepting ability of the hydride hydrogen of **1** was determined using the “rule of factors” proposed by Iogansen<sup>[29]</sup> for organic systems [Equation (3)], where  $P_i$  is the proton-donating ability from Table 2,<sup>[29]</sup> i.e.  $-\Delta H_{11} = 4.6\text{ kcal}\cdot\text{mol}^{-1}$  for the phenol/ethyl ether pair in  $\text{CH}_2\text{Cl}_2$ , with  $P_1 = E_1 = 1.0$ .

$$-\Delta H_{ij} = -\Delta H_{11}P_iE_j \quad (3)$$

The basicity factor ( $E_j$ ) is independent of the proton donor and solvent and for **1** is equal to  $1.37 \pm 0.09$ . Thus, it is possible to compare the proton-accepting ability of **1** with those of boron complexes, some transition metal hydrides and even with organic bases (Table 3).

Table 3. Basicity factors of hydride ligands of  $\text{GaH}_4$ , boron and transition metal hydrides and some organic bases

Compound	$E_j$	Ref.	Compound	$E_j$	Ref.
$\text{GaH}_4^-$	1.37	this work	$[(\text{CH}_2\text{CH}_2\text{PPh}_2)_3\text{FeH}_2]$	1.0	[9]
$\text{BH}_4^-$	1.25	[15]	$[(\text{CH}_2\text{CH}_2\text{PPh}_2)_3\text{RuH}_2]$	1.33	[9]
$[\text{B}_{12}\text{H}_{12}]^{2-}$	0.61	[32]	$[\text{MeC}(\text{CH}_2\text{PPh}_2)_3(\text{CO})\text{RuH}_2]$	1.39	[33]
$[\text{B}_{10}\text{H}_{10}]^{2-}$	0.78	[32]	$[(\text{CH}_2\text{CH}_2\text{PPh}_2)_3\text{OsH}_2]$	1.66	[9]
$\text{Et}_3\text{NBH}_3$	0.53	[15]	DMSO	1.27	[29]
$\text{P}(\text{OEt})_3\text{BH}_3$	0.41	[15]	Py	1.67	[29]

The  $E_j$  value of **1**, as one can see from Table 3, is significantly larger than those of the neutral boron hydrides and even of  $\text{BH}_4^-$  ( $E_j = 1.25$ ), i.e. the proton-accepting ability of hydride ligands increases down the group (B)–H < (Ga)–H. The proton-accepting ability of **1** is close to that of the strongest transition metal hydrides (and organic bases) known to date.<sup>[1,6,15]</sup> The transition metal hydrides with larger basicity factors ( $E_j > 1.5$ ) undergo complete proton transfer from weak XH acids (fluorinated alcohols) to the hydride ligand.<sup>[1,6,9]</sup> Thus, the ease of proton transfer and alcoholysis during the interaction of **1** with



$\text{FCH}_2\text{CH}_2\text{OH}$  and especially  $\text{F}_3\text{CCH}_2\text{OH}$ , in contrast to  $\text{BH}_4^-$ , could be due to the larger proton accepting ability of  $\text{GaH}_4^-$  compared with that of  $\text{BH}_4^-$ .

### Computational Study

A theoretical investigation of the model complexes  $\text{GaH}_4^-\cdot\text{H}_2\text{O}$  (**5**),  $\text{GaH}_4^-\cdot 2\text{H}_2\text{O}$  (**5'**),  $\text{GaH}_4^-\cdot\text{CH}_3\text{OH}$  (**6**),  $\text{GaH}_4^-\cdot\text{CF}_3\text{OH}$  (**7**),  $\text{GaH}_4^-\cdot\text{CF}_3\text{NH}_2$  (**8**) and  $\text{GaH}_4^-\cdot\text{O}_2\text{NC}_6\text{H}_4\text{NH}_2$  (**9**) was performed using the B3LYP approximation with the standard basis set 6-311G(d,p) (see Exp. Sect.). In order to establish the role of the central atom, the model complexes  $\text{BH}_4^-\cdot\text{H}_2\text{O}$  (**10**),  $\text{BH}_4^-\cdot\text{CH}_3\text{OH}$  (**11**) and  $\text{BH}_4^-\cdot\text{CF}_3\text{OH}$  (**12**) were calculated with the 6-311++G(d,p) basis set. This basis set was chosen because of better agreement between the calculated and experimental  $\nu(\text{BH})$  frequencies.

### Structures of DHB Complexes

The results from the theoretical studies are in agreement with the experimental results, showing that the hydride ligand is a proton-accepting site in all cases. There are two types of XH acids. The first type involves the XH acids with only one proton available for donation ( $\text{CH}_3\text{OH}$ ,  $\text{CF}_3\text{OH}$ ). The XH acids of the second group possess two H atoms ( $\text{H}_2\text{O}$ ,  $\text{CF}_3\text{NH}_2$ ,  $4\text{-O}_2\text{NC}_6\text{H}_4\text{NH}_2$ ). Therefore, the possibility of mono- or bidentate coordination for the last proton donor group was considered.

A linear arrangement of the triatomic  $\text{HX}\cdots\text{H}(\text{Ga})$  moiety for the first proton donor group was found (Table 4). The  $\text{X}-\text{H}\cdots\text{H}$  angles are close to  $180^\circ$  ( $170.6^\circ$ ,  $174.6^\circ$  and  $165.8^\circ$  for **6**, **7** and **9**, respectively) and, as was shown earlier, this is typical for classical H-bonding and DHB complexes  $\text{MH}\cdots\text{HX}$  and  $\text{BH}\cdots\text{HX}$ .<sup>[1,6,15]</sup> The  $\text{H}\cdots\text{H}$  distances are smaller than the sum of van der Waals radii ( $2.4 \text{ \AA}$ ) and decrease for stronger alcohols (from  $1.639 \text{ \AA}$  for **6** to  $1.328 \text{ \AA}$  for **7**) (Table 4, Figure 5). Experimentally obtained  $\text{H}\cdots\text{H}$

distances for  $\text{MH}\cdots\text{HX}$  are in the range of  $1.65\text{--}2.1 \text{ \AA}$ .<sup>[1,6]</sup> In the case of the neutral dimer  $(\text{NH}_2\text{HGaH}\cdots\text{HNHGaH}_2)$ , this distance in the crystal is equal to  $1.9 \text{ \AA}$ .<sup>[2]</sup> Therefore, the  $\text{H}\cdots\text{H}$  distance obtained for **7** ( $1.328 \text{ \AA}$ ) is probably too short.

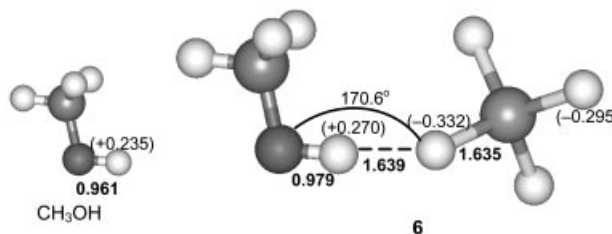


Figure 5. The geometries [ $\text{\AA}$  and  $^\circ$ ] and Mulliken charges (in parentheses) of the model complex  $\text{GaH}_4^-\cdot\text{CH}_3\text{OH}$  (**6**)

The formation of the  $\text{H}\cdots\text{H}$  hydrogen bond leads to the elongation of the  $\text{Ga}-\text{H}$  and  $\text{O}-\text{H}$  bond lengths from their values in the isolated molecules. For example,  $r(\text{Ga}-\text{H}) = 1.622 \text{ \AA}$  in **1** and  $1.635 \text{ \AA}$  in complex **6**,  $r(\text{O}-\text{H}) = 0.961 \text{ \AA}$  in  $\text{CH}_3\text{OH}$  and  $0.979 \text{ \AA}$  in **6**. These changes are close to those previously reported for  $\text{MH}\cdots\text{HX}$  and  $\text{BH}\cdots\text{HX}$  complexes.<sup>[1,6,15]</sup> However, the  $\text{H}\cdots\text{H}$  distance in **6** ( $1.639 \text{ \AA}$ ) is shorter and the value of  $\Delta r(\text{Ga}-\text{H}) = 0.013 \text{ \AA}$  is larger than the corresponding values in complex **11** [ $r(\text{H}\cdots\text{H}) = 1.654 \text{ \AA}$  and  $\Delta r(\text{B}-\text{H}) = 0.005 \text{ \AA}$ ]. The increase in the elongations of the OH bonds is dependent of the OH acid strength (about three times when the  $\text{CH}_3$  group (**6**, **11**) is substituted by  $\text{CF}_3$  (**7**, **12**), Table 4).

Interesting results were obtained for the second group of XH acids. The minima on the potential energy surfaces for  $\text{H}_2\text{O}$  and  $\text{CF}_3\text{NH}_2$  are achieved for bidentate coordination when the two hydride atoms of **1** interact with both hydrogen atoms of the  $\text{XH}_2$  groups forming a symmetrical chelated structure (Figure 6). The interaction between these species leads to nonlinear  $\text{OH}\cdots\text{H}$  and  $\text{NH}\cdots\text{H}$  moieties and

Table 4. The characteristics of DHB complexes calculated by the DFT method

	Model complex	Angle $\text{H}\cdots\text{HX}$ [ $^\circ$ ]	$r(\text{H}\cdots\text{H})$ [ $\text{\AA}$ ]	$\Delta r$ (EH) [ $\text{\AA}$ ]	$\Delta r$ (XH) [ $\text{\AA}$ ]	$\Delta q\text{H}$ (EH)	$\Delta q\text{H}$ (XH)	$-\Delta H$ [ $\text{kcal}\cdot\text{mol}^{-1}$ ]	$-\Delta H$ per H bond [ $\text{kcal}\cdot\text{mol}^{-1}$ ]
<b>5</b>	$\text{GaH}_4^-\cdot\text{H}_2\text{O}$	147.5	2.005 0.028	0.007	0.006	0.019	0.010	10.7	5.4
<b>5'</b>	$\text{GaH}_4^-\cdot 2\text{H}_2\text{O}$	147.2	2.032 0.024	0.003	0.006	0.001	0.010	20.4	5.1
<b>6</b>	$\text{GaH}_4^-\cdot\text{CH}_3\text{OH}$	170.6	1.639 0.074	0.013	0.018	0.018	0.035	9.1	
<b>7</b>	$\text{GaH}_4^-\cdot\text{CF}_3\text{OH}$	174.6	1.328 0.190	0.034	0.064	0.020	0.022	19.6	
<b>8</b>	$\text{GaH}_4^-\cdot\text{CF}_3\text{NH}_2$	140.8	2.047 0.044	0.011	0.008	0.018	0.010	12.6	6.3
<b>9</b>	$\text{GaH}_4^-\cdot\text{O}_2\text{NC}_6\text{H}_4\text{NH}_2$	165.8	1.755 0.098	0.021	0.021	0.019	0.034	17.9	
<b>10</b>	$\text{BH}_4^-\cdot\text{H}_2\text{O}$	174.5	1.690 0.152	0.006	0.019	0.044	0.038	11.6	
<b>11</b>	$\text{BH}_4^-\cdot\text{CH}_3\text{OH}$	172.8	1.654 0.174	0.005	0.021	0.032	0.014	11.13	
<b>12</b>	$\text{BH}_4^-\cdot\text{CF}_3\text{OH}$	164.6	1.350	0.014	0.072	0.075	0.049	24.02	

induces less bond elongation. The H...H distances are longer than in the complexes of the first group (Table 4).

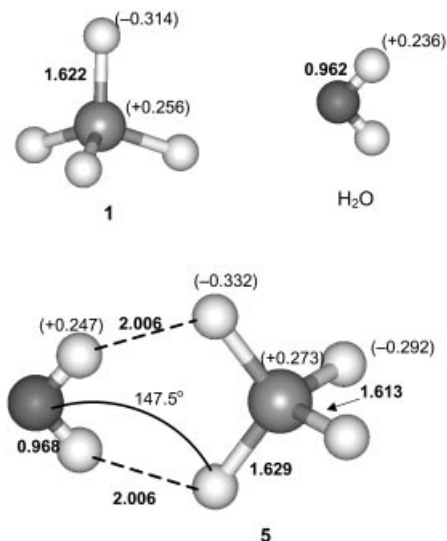


Figure 6. The geometries [Å and °] and Mulliken charges (in parentheses) of the model complex  $\text{GaH}_4^- \cdot \text{H}_2\text{O}$  (**5**)

Thus, the DHB complexes **5** (Figure 6) and **8** exhibit longer H...H distances (2.005 and 2.047 Å) than for **6** and **7**, smaller elongations (0.007–0.011 Å) and more acute O–H...H and N–H...H angles (147.5° and 140.8°, respectively). Interaction with the second water molecule leads to complex **5'** with a second symmetrical chelated ring and practically the same OH...H angle. Only the Ga–H elongations are less (in 0.004 Å) and the H...H distance is a little larger (in 0.027 Å) compared with that in **5**.

It was found that the differences in the structures of the  $\text{EH}_4^- \cdot \text{H}_2\text{O}$  complexes depend on the central atom. The monodentate coordination of  $\text{H}_2\text{O}$  is characteristic for  $\text{BH}_4^- \cdot \text{H}_2\text{O}$  (**10**) instead of the symmetrical chelate structure of **5** (Figure 6). The O–H...H angle of **10** (174.5°) is larger than in **5** and is close to 180°. The additional interaction between the free hydride atoms of  $\text{BH}_4^-$  and the free hydrogen atom in the water molecule<sup>[15]</sup> should not be regarded as the second H bond because the H...H distance is equal to 2.48 Å. This is larger than the sum of the van der Waals radii.

Reducing the proton donor strength by substitution of R in  $\text{RNH}_2$  from  $\text{CF}_3$  in **8** to 4- $\text{O}_2\text{NC}_6\text{H}_4$  in **9** also leads to monodentate coordination of the proton donor with an additional interaction of the second acidic hydrogen atom similar to the situation in **10**. This additional interaction can also not be regarded as a DHB bond (H...H distance = 2.449 Å; Figure 7).

The increase of the N–H...H angle (165.8°), the additional lengthening of the Ga–H and O–H bonds (0.021, 0.021 Å) and the shortening of the H...H distance (1.755 Å) are characteristic for **9** when compared with **8**.

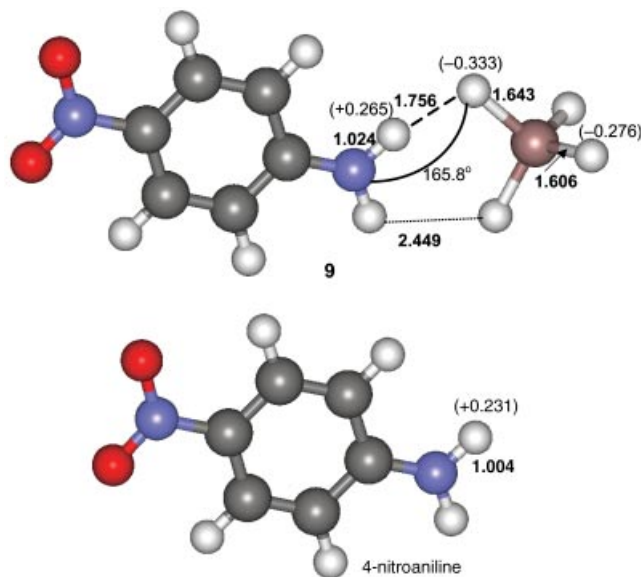


Figure 7. The geometries [Å and °] and Mulliken charges (in parentheses) of the model complex  $\text{GaH}_4^- \cdot \text{O}_2\text{NC}_6\text{H}_4\text{NH}_2$  (**9**)

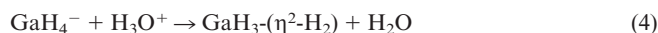
### Energies of DHB Complexes and Electron Density Changes

The calculated energy values of the complexes (Table 4) are larger than those obtained experimentally. For example, the energy of  $\text{GaH}_4^- \cdot \text{CH}_3\text{OH}$  (**6**) is about twice as high as the enthalpy value obtained from Equations (2) and (3) from IR spectroscopic data (Table 2). The probable cause of such overestimation may be the decrease of the DHB energy on going from the gas phase (calculations) to solution (experimental measurements).<sup>[6,15]</sup> As was indicated previously, the significant solvation effects are related to ion-molecular H bonds due to the significantly larger solvation energies for anions over hydrogen-bonded complexes.<sup>[34]</sup> Note, however, that the energy overestimation is more for  $\text{BH}_4^- \cdot \text{HOR}$  complexes. This could be explained by the smaller dimension and greater solvation effect of  $\text{BH}_4^-$  in comparison with  $\text{GaH}_4^-$ .<sup>[34]</sup> It is remarkable that the calculated energy values for the linear monodentate complexes (9.1–19.6 kcal·mol<sup>−1</sup>) are higher than for the bidentate nonlinear DHBs (5.35–6.3 kcal·mol<sup>−1</sup> per bond). The energy increase is dependent on the XH acid strength, for example, **6** < **7** (Table 4).

The overlap populations (*o.p.*) of the H...H bonds and the electron redistribution upon DHB formation also depend on the type of coordination and the acid strength. The *o.p.* of the H...H bonds vary in the range of 0.016–0.095 and their values are larger in the case of linear monodentate coordination. Small but positive overlap populations indicative of the covalent component of DHB increase upon going from **6** to **7**. The electrostatic attraction between the partial negative charge of the hydrogen atom of  $\text{GaH}_4^-$  (−0.314) and partial positive charge of the proton donors (from 0.22 to 0.27 dependent on their strength) is the driving force for dihydrogen bonding  $\text{GaH}_4^{\delta-} \cdots \text{H}^{\delta+}\text{X}$  as was previously determined for  $\text{MH}_4^{\delta-} \cdots \text{H}^{\delta+}\text{X}$ .<sup>[1,6]</sup> DHB formation leads to an increase of the charges which is a little

more substantial in the case of the monodentate complexes, especially for the hydrogen atom of the XH acids [for example,  $\Delta q\text{H}(\text{OH}) = 0.035$  for **6** and  $\Delta q\text{H}(\text{OH}) = 0.010$  for **5**] (Table 4).

The calculation of the interaction of **1** with a strong acid shows the proton transfer reaction leading to the dihydrogen complex formation [Equation (4)].



Upon proton transfer to a hydride ligand, the tetrahedron of **1** transforms in to the planar gallium trihydride with the side on ( $\eta^2\text{-H}_2$ ) ligand (Figure 8). The H–H distance is equal to 0.756 Å which is a little longer than in the  $\text{H}_2$  molecule (0.74 Å) and shorter than in transition metal dihydrogen complexes (0.8–1.1 Å).<sup>[1,4,6]</sup> The large energy calculated ( $167.16 \text{ kcal}\cdot\text{mol}^{-1}$ ) is in agreement with Equation (4) which demands significant electron and structural reorganization. Such an unstable dihydrogen complex was predicted theoretically and observed experimentally by IR matrix isolation in the case of boron.<sup>[28]</sup>

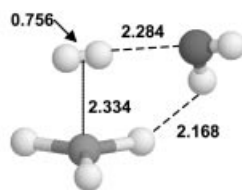


Figure 8. The geometries [Å] of the unstable products of the proton transfer reaction (4)

### Spectroscopic Characteristics of DHB Complexes

The calculated spectroscopic characteristics of the complexes (stretching vibrations of X–H and Ga–H bonds) are presented in Table 5. The  $\nu(\text{XH})_{\text{bonded}}$  bands are shifted to the low-frequency range in agreement with the experimental observations. The values of the shifts depend on the strength of the XH acid and the linearity of the X–H $\cdots$ H moiety. Linear bonds result in larger  $\nu$  values. The value of  $\nu(\text{OH})$  in complex **6** is about twice as large as in nonlinear **5**, although the acidity of methanol and water are similar ( $\text{p}K_{\text{a}} \approx 15.5$ ). The  $\nu(\text{OH})$  value depends on the proton-donating ability in the sequence:  $\text{F}_3\text{COH} > \text{CH}_3\text{OH} > \text{NO}_2\text{C}_6\text{H}_4\text{NH}_2 > \text{H}_2\text{O} \geq \text{CF}_3\text{NH}_2$ .

The bands of the free Ga–H groups in the complexes increase in agreement with the experimental IR spectroscopic changes observed for DHB complexes with **1**, the boron analogue<sup>[15]</sup> and transition metal hydrides.<sup>[6]</sup>

Hence, the calculations reproduced the main structural features and the charge redistribution occurring as a result of hydrogen-bond formation as a function of the proton-donor strength and the type of coordination.

### Conclusion

The present variable-temperature IR investigation of the interaction between  $\text{GaH}_4^-$  and different XH acids shows for the first time the  $\text{GaH}\cdots\text{HX}$  dihydrogen-bond formation in solution. The spectroscopic characteristics, DHB formation enthalpies with different XH acids and the  $E_{\text{f}}$  factors of  $\text{GaH}_4^-$  were determined and appear to be greater than those of the boron analogue DHB, demonstrating an increase in the proton-accepting ability down the group. Two types of DHB model complexes were determined from DFT calculations: the linear monodentate with XH acids or 4-nitroaniline and the nonlinear bidentate with  $\text{XH}_2$  acids containing symmetrical chelate hydrogen bonds to two hydride atoms of **1**. This last type of DHB was not found for  $\text{BH}_4$  and is specific to the  $\text{GaH}_4^-$  anion. It was shown that the elongation of the bonds of the  $\text{GaH}\cdots\text{HX}$  moiety, polarisation of the partners and the energy depend on the type of coordination and the strength of the X–H acids.

A study of a number of group 13 hydride DHB complexes would be of great interest for determining the  $\text{EH}\cdots\text{HX}$  energies and structures as a function of the position of the group 13 element, as well as the mechanisms of aminolysis and alcoholysis through DHB. We are currently investigating these issues.

### Experimental Section

The  $[\text{Bu}_4\text{N}][\text{GaH}_4]$  salt (**1**) was prepared as described in the literature.<sup>[36]</sup> Fluorinated alcohols were provided by P&M (Moscow, Russia). The solutions for IR studies were prepared under argon by standard Schlenk technique. Tetrahydrofuran (THF) was freshly distilled from  $\text{LiAlH}_4$  and  $\text{CH}_2\text{Cl}_2$  was purified by distillation from  $\text{CaH}_2$  before use. The anhydrous solvents were thoroughly degassed prior to use.

Table 5. Calculated  $\nu(\text{XH})$  and  $\nu(\text{GaH})$  frequencies for the model complexes [ $\text{cm}^{-1}$ ]

	Model complex	$\nu(\text{XH})_{\text{free}}^{[a]}$	$\nu(\text{XH})_{\text{bond}}^{[a]}$	$\Delta\nu(\text{XH})^{[a]}$	$\nu(\text{GaH})_{\text{free}}$	$\nu(\text{GaH})_{\text{bond}}$	$\Delta\nu(\text{GaH})^{[b]}$
<b>5</b>	$\text{GaH}_4^-\cdot\text{H}_2\text{O}$	3672 (as)	3532	140	1739	1656	37
<b>6</b>	$\text{GaH}_4^-\cdot\text{CH}_3\text{OH}$	3607	3278	329	1719	1669	24
<b>7</b>	$\text{GaH}_4^-\cdot\text{CF}_3\text{OH}$	3591	2486	1105	1766	1688	5
<b>8</b>	$\text{GaH}_4^-\cdot\text{CF}_3\text{NH}_2$	3415 (as)	3281	134	1739	1636	57
<b>9</b>	$\text{GaH}_4^-\cdot\text{O}_2\text{NC}_6\text{H}_4\text{NH}_2$	3409 (s)	3124	285	1757	1677	16
		3521 (as)					

<sup>[a]</sup> The values are presented by a scaling factor 0.94.<sup>[35]</sup> <sup>[b]</sup>  $\Delta\nu(\text{GaH}) = \nu(\text{GaH})_{\text{initial}} - \nu(\text{GaH})_{\text{bond}} = 1693 - \nu(\text{GaH})_{\text{bond}}$ .

Table 6. Comparative analysis of the frequencies [ $\text{cm}^{-1}$ ], energy [ $\text{kcal}\cdot\text{mol}^{-1}$ ], Mulliken charges and overlap population of  $\text{GaH}_4^-$ , calculated with different basis sets

B3LYP/ basis set	6-31G(d,p)	6-31++G(d,p)	6-311G(d,p)	6-311+G(d,p)	6-311++G(d,p)	$\nu(\text{exp})^{[a]}$
$\nu_i$ (calcd.)	737.1 800.1 1795.3 1847.5	744.2 802.5 1780.8 1846.6	731.9 786.3 1693.6 1766.7	731.6 785.7 1690.1 1765.9	729.7 781.4 1685.2 1762.7	733 (780) 1700 <sup>[b]</sup> 1770
$E_{\text{terminal}}$	17.855	17.823	17.251	17.233	17.19	
$q_{\text{Ga}}$	-0.516	0.095	0.256	0.252	0.408	
$q_{\text{H}}$	-0.121	-0.274	-0.314	-0.313	-0.352	
Overlap population	0.800	0.707	0.716	0.716	0.695	

<sup>[a]</sup> IR, Raman frequencies of  $\text{CsGaH}_4$  in diglyme solution.<sup>[39]</sup> <sup>[b]</sup> IR frequency of  $\nu(\text{GaH})$   $\text{Bu}_4\text{NGaH}_4$  in THF solution:  $1696\text{ cm}^{-1}$ .

The IR spectra of THF or  $\text{CH}_2\text{Cl}_2$  solutions (cells  $\text{CaF}_2$ ,  $d = 0.012$ – $0.120\text{ cm}$ ) were measured with a Specord M-82 (Carl Zeiss Jena) spectrometer with a  $2$ – $4\text{ cm}^{-1}$  resolution. The low-temperature IR studies were carried out in the OH and GaH stretching regions using a Carl Zeiss Jena cryostat in the temperature range of  $200$ – $300\text{ K}$  with the accuracy of the temperature setting being  $\pm 0.5\text{ K}$ . Concentrations of  $[\text{Bu}_4\text{N}][\text{GaH}_4]$  were varied from  $10^{-1}$  to  $10^{-2}\text{ M}$  in the range of  $\nu(\text{XH})$  to  $10^{-2}$  to  $10^{-3}\text{ M}$  in the range of  $\nu(\text{GaH})$ . The concentrations of the XH acids in the first range were between  $10^{-2}$  and  $10^{-3}\text{ M}$  or between  $10^{-1}$  to  $10^{-2}\text{ M}$  in the range of  $\nu(\text{GaH})$ .

The theoretical calculations of the model complexes  $\text{GaH}_4^-\cdot\text{H}_2\text{O}$ ,  $\text{GaH}_4^-\cdot\text{CH}_3\text{OH}$ ,  $\text{GaH}_4^-\cdot\text{CF}_3\text{OH}$ ,  $\text{GaH}_4^-\cdot\text{CF}_3\text{NH}_2$ , and  $\text{GaH}_4^-\cdot\text{NO}_2\text{C}_6\text{H}_4\text{NH}_2$  were performed by the hybrid density functional method<sup>[37]</sup> with the Gaussian 98 series of programs.<sup>[38]</sup> Firstly, several basis sets were used to perform the  $\text{GaH}_4^-$  calculations (Table 6).

Finally, the choice of the basis set was made based on good agreement between the calculated and experimental  $\nu(\text{GaH})$  frequencies. For the first two basis sets [6-31G(d,p) and 6-31++G(d,p)]  $\Delta\nu(\text{GaH}) = \nu(\text{GaH})_{\text{exp}} - \nu(\text{GaH})_{\text{calcd.}}$  values were too large ( $101.7$  and  $87.2\text{ cm}^{-1}$ , respectively), while for the 6-311G(d,p) basis set they were equal to  $6.4^{[39]}$  or  $2.6\text{ cm}^{-1}$  (this work). The basis set chosen [6-311G(d,p)] is also better for the electron-density description, giving the positive charge on Ga (as for B in the boron analogue)<sup>[15,16]</sup> though the Ga atom has either negative, or near to zero charge with the first two poorer basis sets. The higher computational levels increased the time of computations but practically did not improve the results. Therefore, the basis set 6-311G(d,p) was chosen for further calculations of the above-mentioned complexes  $1\cdot\text{HX}$ .

## Acknowledgments

This work was supported by European Commission's RTN Programme "HYDROCHEM" (HPRN-CT-2002-00176), the Russian Foundation for Basic Research (02-03-32068, 03-03-06277, 04-03-32456) and the Fundamental Research Program of the RAS Presidium.

- <sup>[1]</sup> L. M. Epstein, E. S. Shubina, *Coord. Chem. Rev.* **2002**, *231*, 165.  
<sup>[2]</sup> E. S. Shubina, N. V. Belkova, L. M. Epstein, *J. Organomet. Chem.* **1997**, *17*, 536–537.  
<sup>[3]</sup> J. C. M. Rivas, L. Brammer, *Coord. Chem. Rev.* **1999**, *43*, 183.  
<sup>[4]</sup> R. H. Morris, in *Recent Advances in Hydride Chemistry*, Elsevier, Amsterdam, **2001**, p. 3.  
<sup>[5]</sup> E. Clot, O. Eisenstein, D.-H. Lee, R. H. Crabtree, in *Recent Advances in Hydride Chemistry*, Elsevier, Amsterdam, **2001**, p. 75.

- Advances in Hydride Chemistry*, Elsevier, Amsterdam, **2001**, p. 75.  
<sup>[6]</sup> L. M. Epstein, N. V. Belkova, E. S. Shubina, in *Recent Advances in Hydride Chemistry*, Elsevier, Amsterdam, **2001**, p. 391.  
<sup>[7]</sup> I. Alcorta, I. Rozas, J. Elguero, *J. Mol. Struct.* **2001**, *537*, 139.  
<sup>[8]</sup> F. Maseras, A. Lledos, E. Clot, O. Eisenstein, *Chem. Rev.* **2000**, *100*, 615.  
<sup>[9]</sup> E. I. Gutsul, N. V. Belkova, M. S. Sverdlov, L. M. Epstein, E. S. Shubina, V. I. Bakhmutov, T. N. Gribova, R. M. Minyaev, C. Bianchini, M. Peruzzini, F. Zanobini, *Chem. Eur. J.* **2003**, *2219*.  
<sup>[10]</sup> N. V. Belkova, A. V. Ionidis, L. M. Epstein, E. S. Shubina, St. Gruendemann, N. S. Golubev, H.-H. Limbach, *Eur. J. Inorg. Chem.* **2001**, 1753.  
<sup>[11]</sup> N. V. Belkova, L. M. Epstein, A. Lledos, F. Maseras, E. S. Shubina, *J. Am. Chem. Soc.* **2003**, *125*, 7715.  
<sup>[12]</sup> T. B. Richardson, S. de Gala, R. H. Crabtree, P. E. M. Siegbahn, *J. Am. Chem. Soc.* **1995**, *117*, 12875.  
<sup>[13]</sup> R. H. Crabtree, P. E. M. Siegbahn, O. Eisenstein, A. L. Rheingold, T. F. Koetzle, *Acc. Chem. Res.* **1996**, *29*, 348.  
<sup>[14]</sup> E. S. Shubina, E. V. Bakhmutova, L. M. Epstein, *Mendeleev Commun.* **1997**, 87.  
<sup>[15]</sup> L. M. Epstein, E. S. Shubina, E. V. Bakhmutova, L. N. Saitkulova, V. I. Bakhmutov, A. L. Chistyakov, I. V. Stankevich, *Inorg. Chem.* **1998**, *37*, 3013.  
<sup>[16]</sup> P. L. A. Popelier, *J. Phys. Chem. A* **1998**, *102*, 1873.  
<sup>[17]</sup> C. J. Cramer, W. L. Gladfelter, *Inorg. Chem.* **1997**, *36*, 5358.  
<sup>[18]</sup> W. T. Kloster, T. F. Koetzle, P. E. M. Siegbahn, T. B. Richardson, R. H. Crabtree, *J. Am. Chem. Soc.* **1999**, *121*, 6337.  
<sup>[19]</sup> I. Alcorta, I. Rozas, J. Elguero, *Chem. Soc. Rev.* **1998**, *27*, 163.  
<sup>[20]</sup> R. Coustecean, J. E. Jackson, *Chem. Rev.* **2001**, *101*, 1963.  
<sup>[21]</sup> S. Aldridge, A. J. Downs, *Chem. Rev.* **2001**, *101*, 3305.  
<sup>[22]</sup> S. J. Grabowski, *Chem. Phys. Lett.* **1999**, *312*, 542.  
<sup>[23]</sup> J. P. Campbell, J. W. Hwang, W. G. Young, R. B. Dreele, C. J. Cramer, W. L. Gladfelter, *J. Am. Chem. Soc.* **1998**, *120*, 521.  
<sup>[24]</sup> J. L. Atwood, G. A. Koutsantonis, G. A. Lee, C. L. Raston, *J. Chem. Soc., Chem. Commun.* **1994**, 91.  
<sup>[25]</sup> G. N. Patwari, T. Ebata, N. Mikami, *Chem. Phys.* **2002**, *283*, 193.  
<sup>[26]</sup> J. Golden, C. Schreier, B. Singaram, S. Williamson, *Inorg. Chem.* **1992**, *31*, 1533.  
<sup>[27]</sup> V. V. Gavrilenko, V. S. Kolesov, L. I. Zakharkin, *Russ. Chem. Bull.* **1984**, 2766.  
<sup>[28]</sup> P. R. Schreiner, H. F. Schaefer, P. v. R. Schleyer, *J. Chem. Phys.* **1994**, *101*, 7625.  
<sup>[29]</sup> A. V. Iogansen, *Theor. Experim. Khim.* **1971**, *7*, 302 and 314.  
<sup>[30]</sup> A. V. Iogansen, *The Hydrogen Bond*, Nauka, Moscow, **1981**, p. 134.  
<sup>[31]</sup> A. V. Iogansen, *Spectrochim. Acta A* **1999**, *55*, 1585.  
<sup>[32]</sup> E. S. Shubina, E. V. Bakhmutova, A. M. Filin, I. B. Sivaev, L. N. Teplitskaya, A. L. Chistyakov, I. V. Stankevich, V. I.



- Bakhmutov, V. I. Bregadze, L. M. Epstein, *J. Organomet. Chem.* **2002**, 657, 155.
- [33] V. I. Bakhmutov, E. V. Bakhmutova, N. V. Belkova, C. Bianchini, L. M. Epstein, M. Peruzzini, E. S. Shubina, E. V. Vorontsov, F. Zanobini, *Can. J. Chem.* **2001**, 79, 479.
- [34] L. M. Epstein, L. N. Saitkulova, E. S. Shubina, *J. Mol. Struct.* **1992**, 270, 325.
- [35] G. Rauhut, P. Pulay, *J. Phys. Chem.* **1995**, 99, 3093.
- [36] L. I. Zakharkin, V. V. Gavrilenko, Yu. N. Karaksin, *Synt. Inorg. Metal-Org. Chem.* **1971**, 1, 37.
- [37] A. D. Becke, *J. Chem. Phys.* **1993**, 98, 5648.
- [38] M. J. Frisch, G. W. Trucks, H. B. Schlegel, G. E. Scuseria, M. A. Robb, J. R. Cheeseman, V. G. Zakrzewski, J. A. Montgomery, Jr., R. E. Stratmann, J. C. Burant, S. Dapprich, J. M. Millam, A. D. Daniels, K. N. Kudin, M. C. Strain, O. Farkas, J. Tomasi, V. Barone, M. Cossi, R. Cammi, B. Mennucci, C. Pomelli, C. Adamo, S. Clifford, J. Ochterski, G. A. Petersson, P. Y. Ayala, Q. Cui, K. Morokuma, D. K. Malick, A. D. Rabuck, K. Raghavachari, J. B. Foresman, J. Cioslowski, J. V. Ortiz, A. G. Baboul, B. B. Stefanov, G. Liu, A. Liashenko, P. Piskorz, I. Komaromi, R. Gomperts, R. L. Martin, D. J. Fox, T. Keith, M. A. Al-Laham, C. Y. Peng, A. Nanayakkara, M. Challacombe, P. M. W. Gill, B. Johnson, W. Chen, M. W. Wong, J. L. Andres, C. Gonzalez, M. Head-Gordon, E. S. Replogle, and J. A. Pople, *Gaussian 98, Revision A.9*, Gaussian, Inc., Pittsburgh PA, **1998**.
- [39] A. P. Kurbakova, L. A. Leites, V. V. Gavrilenko, Yu. N. Karaksin, L. I. Zakharkin, *Spectrochim. Acta, Sect. A* **1975**, 31, 281.

Received February 2, 2004

Early View Article

Published Online June 23, 2004